Available at
http://pvamu.edu/aam
Appl. Appl. Math.
ISSN: 1932-9466

Applications and Applied Mathematics:
An International Journal
(AAM)

Vol. 13, Issue 2 (December 2018), pp. 952 – 974

Parameter Estimation and Optimal Control of the Dynamics Of Transmission of Tuberculosis with Application to Cameroon

[1]A. Temgoua, [2,5]Y. Malong, [3,5]J. Mbang and [4,5,*]S. Bowong

[1,2,4] Laboratory of Mathematics
Department of Mathematics and Computer Science
Faculty of Science
University of Douala
PO Box 24157
Douala, Cameroon
[1]anatoletemgoua@yahoo.fr; [2]ycmalong@yahoo.fr; [4]sbowong@univ-douala.com

[3] Department of Mathematics
University of Yaounde I
PO Box 812
Yaounde, Cameroon
[3]mbangjoh@yahoo.fr

[5] UMI 209 IRD & UPMC UMMISCO
Bondy, France
Project team GRIMCAPE-Cameroon
The African Center of Excellence in Information and Communication Technologies (CETIC)
University of Yaounde 1
Cameroon

*Corresponding Author

Received: November 22, 2017; Accepted: May 28, 2018

Abstract

This paper deals with the problem of parameter estimation and optimal control of a tuberculosis (TB) model with seasonal fluctuations. We first present a uncontrolled TB model with seasonal fluctuations. We present the theoretical analysis of the uncontrolled TB model without seasonal fluctuations. After, we propose a numerical study to estimate the unknown parameters of the TB model with seasonal fluctuations according to demographic and epidemiological data from

Cameroon. Simulation results are in good accordance with the seasonal variation of the new active reported cases of TB in Cameroon. Using this TB model with seasonality, the tuberculosis control is formulated and solved as an optimal control problem, indicating how control terms on the chemoprophylaxis and treatment should be introduced in the considered TB model to reduce the number of individuals with active TB. Results provide a framework for designing cost-effective strategies for TB with two strategies of intervention.

Keywords: Epidemiological models; Tuberculosis; DOTS strategy; Season pattern; Optimal control

MSC 2010 No.: 34A34, 34D23, 34D40, 92D30

1. Introduction

Disease spreading has been the subject of intense research since a long time ago (Anderson et al. (1992), Daley et al. (1999), Murray (2002)). Our current knowledge comprises mathematical models that have allowed to better understand how an epidemic spreads and to design more efficient immunization and vaccination policies (Anderson et al. (1992), Daley et al. (1999), Murray (2002)). These models have gained in complexity in recent years capitalizing on data collections which have provided information on the local and global patterns of relationships in the population (Hufnagel et al. (2004), Guimera et al. (2005), Colizza et al. (2006)). However, despite significant advances in medical science, infectious diseases continue to impact human populations in many parts of the world.

Tuberculosis is a common deadly infectious disease caused mainly by the *Mycobacterium tuberculosis* (*M. tuberculosis*). It basically attacks the lungs (pulmonary TB), but can also affect the central nervous system, the circulatory system, the genital-urinary system, bones, joints and even the skin. Tuberculosis can spread through cough, sneeze, speak, kiss or spit from active pulmonary TB persons. It can also spread through using of an infected person's unsterilized eating utensils and in rare cases a pregnant woman with active TB can infect her fetus (vertical transmission) (see WHO (2009) and Bleed et al. (1982)). The current world estimate of prevalence is about 33%, while the number of deaths per year that it is causing reaches more than 3 million people (WHO (2009).

Depending on the kind and the intensity of immune response that the host immune system performs after initial infection with the *M. tuberculosis* bacillus, the individual can suffer latent infection, in which the bacteria are under a growth-arrest regime and the individual neither suffer any clinical symptoms nor becomes infectious or actively infected, where the host suffers clinical symptoms and can transmit the pathogen by air (WHO (2009) and Bleed et al. (1982)). Latently infected individuals can, generally after an immune-depression episode, reach the active phase. Estimating the probability of developing direct active infection after a contact, or alternatively, the lifetime's risk for a latent infected individual to evolve into the active phase, are not easy tasks. However, it is generally accepted that only 5-10% of the infections directly produce active TB (WHO (2009) and Bleed et al. (1982)), while the ranges concerning the estimation of a typical "half-life" of latent state rounds about 500 years (Styblo (1986)).

Although TB is not widely recognized as having seasonal trends like measles, diphtheria, chickenpox, cholera, rotavirus, malaria, or even sexually transmitted gonorrhea (Grassly et al. (2006) and Hethcote et al. (1984)), some studies have shown variable periods of peak seasonality in TB incidence rates in late winter to early spring in South Africa (Murphy et al. (2002)), during summer in United Kingdom (Schaaf et al. (1996)) and Hong Kong (Douglas et al. (1996)), during summer and autumn in Spain (Leung et al. (2005)), and during spring and summer in Japan (Rios et al. (2000)). In the northern India, it was indicated that TB diagnosis peaked between April and June, and reached a nadir between October and December, and the magnitude of seasonal variation had an important positive correlation with rates of new smear-positive TB cases (Nagayama et al. (2006)).

The real causes of seasonal patterns of TB remain unknown, but the seasonal trend, with a higher incidence rate in winter, may be relevant to the increased periods spent in overcrowded, poorly ventilated housing conditions, these phenomena much more easily seen than in warm seasons (Murphy et al. (2002) and Leung et al. (2005)), and/or vitamin D deficiency leading to reactivation of latent/exposed infection, which may have been the basic causes for the observed TB seasonality (Nagayama et al. (2006)). Furthermore, in winter and spring, the viral infections like flu are more frequent and cause immunological deficiency leading to a reactivation of the M. tuberculosis (see Leung et al. (2005)). There is a growing awareness that seasonality can cause population fluctuations ranging from annual cycles to multi year oscillations, and even chaotic dynamics (Nagayama et al. (2006)). From an applied perspective, clarifying the mechanisms that link seasonal environmental changes to diseases dynamics may aid in forecasting the long-term health risks, in developing an effective public health program, and in setting objectives and utilizing limited resources more effectively (see, for instance, Leung et al. (2005) and Aron et al. (1984)). For these reasons, we need to identify possible seasonal patterns in the incidence rate for pulmonary tuberculosis.

Mathematical models play a significant role in understanding the transmission dynamics of TB. Estimation of parameters in a TB mathematical model, for instance, infection rate or reactivation rate can contribute to better quantify the spread of the disease. Generally, inference of these parameters is a difficult task because of poor compatibility between observed data and models. Simulations and epidemiological data have been used to estimate the key parameters of deterministic models. Several methods have been introduced and applied to estimate the parameters of TB models. Approximate Bayesian computation approach has been used to estimate TB transmission rate parameters for United States by Altizer et al. (2006). Liu et al. (2010) estimated the reactivation and infection rates of a TB model for China by assuming these rates as sinusoidal functions and infection rate is estimated to be 2.23 person per month for the period 2005-2009. A synchronisation based method has been implemented to infer the parameters such as treatment rate, disease induced mortality rate and infection rate of a TB model by Bowong et al. (2010). In particular, the infection rate in the study is estimated to be 2.04 for the quarterly data during 2003-2007 for Cameroon. Moualeu et al. (2013) used the iterative Gauss-Newton method to solve the inverse problem of parameter identification, estimability of parameters have been studied, and estimable unknown parameters have been computed using real data of TB in Cameroon, subdivided into four regions. Numerical simulations showed the model to reproduce the TB dynamics in Cameroon and predict a short term increase in the number of TB active cases over next years. Narula et al. (2016)

have estimated parameters of a TB model using Ensemble Kalman filter (EnKf) approach. More precisely, the infection rate and fraction of smear positive cases of TB are estimated in context of India. The infection rate of TB in Manipur is found to be 2.57 per quarter for the period 2006-2011.

On the other hand, mathematical models can provide a powerful tool for investigating the dynamics and control of infectious diseases. Optimal control theory provides a valuable tool to begin to assess the trade-offs between vaccination and treatment strategies (Anderson et al. (1990) and Lenhart et al. (2007)). Optimal control is a mathematical technique derived from the calculus of variations. Anyhow we can give suggestions to the public health authorities about the effects of a particular control policy with respect to others, and in this context the analysis and simulation of mathematical models may become a powerful tool in the hands of the above authorities.

There are a number of different methods for calculating the optimal control for a specific mathematical model. For example, Pontryagin's maximum principle (Pontryagin et al. (1967)) allows the calculation of the optimal control for an ordinary differential equations model system with a given constraint. Variations of Pontryagin's maximum principle have been derived for other types of models including partial differential equations and difference equations (Anderson et al. (1990), Fleming et al. (1975)). These techniques are powerful when applied to disease models and can provide important insights into the best pathway to reduce disease burden. For example, with a given mathematical model for a disease, one can calculate the best vaccination schedule balancing the cost of the vaccine and the cost of the disease burden (see Fleming et al. (1975)). There have been several articles considering optimal control applied to specific diseases (see, for instance, Joshi (2002), Jung et al. (2002), and Wang et al. (2004)). However, none of these papers has included TB seasonality.

The present work considers the parameter estimation as well as the optimal control problem of the dynamics of transmission of tuberculosis with seasonality. We first present an uncontrolled TB model that incorporates the essential biological and epidemiological features of this disease such as the exogenous reinfection and seasonal fluctuations. We present the mathematical analysis of the uncontrolled TB model without seasonality. After, using the quarterly reported data (2003-2007) of the National Committee to Fight against Tuberculosis (NCFAT, (2001)), we estimate the infection and reactivation rates of the TB model with seasonality. Compared to the result obtained by Altizer et al. (2006), Liu et al. (2010), Bowong et al. (2010), Moualeu et al. (2013) and Narula et al. (2016), the advantage of the proposed parameter estimation method is that it is less computationally intensive and easier to implement. We point out that the transmission rate of TB and reactivation rate of latently infected individuals cannot be estimated directly using TB data. So, these parameters are usually unknown parameters. Narula et al. (2016). have estimated the TB transmission rate and the fast rout to active TB. The reactivation rate of latently-infected individuals has not been estimated which is the case in the present work. Also, the transmission and reactivation rates are time-dependent and capture the saison pattern of TB. This is not the case in Narula et al. (2016). In addition, we approach the chemoprophylaxis and treatment problem by posing it as an optimal control problem in which we minimize the benefit based on the levels of latently-infected individuals and infectious, less the systemic cost of chemoprophylaxis and treatment. We found that the infection level decreases to low levels, but is never eradicated. For the best of authors knowledge, this study represents the first work that provides an in-depth TB seasonality, parameter estimation

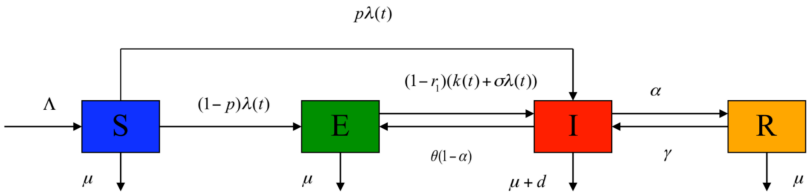

Figure 1. Flowchart of the dynamical transmission of tuberculosis where $\lambda(t) = \beta(t)I/N$ is the force of infection.

and optimal control using real demographic and epidemiological data of the situation of TB in a developing country like Cameroon.

2. The Model

2.1. Model construction

We consider that individuals within a human community are compartmentalized into four groups: heathly-or susceptible-$S(t)$, infected but not infectious-or latently infected $E(t)$, sick individuals $I(t)$ which are infected, and infectious as well-and recovered individuals $R(t)$. Thus, the total population $N(t)$ at time t is $N(t) = S(t) + E(t) + I(t) + R(t)$.

In view of the periodic trend of quarterly new TB cases in Cameroon (NCFAT (2001)) and the possible causes of the seasonal pattern (Liu et al. (2010)), a model with periodic infection and reactivation rates may be a natural choice to describe the TB transmission. Thus, we assume that infection and reactivation rates are periodic positive continuous functions in t with period ω for some $\omega > 0$. The transition between these sub-populations proceeds in such a way that a susceptible individual acquires the bacteria through a contact with an infectious subject with the transmission rate $\beta(t)$. In its turn, this newly infected individual may develop the disease directly with the probability p. However, the most common case is the establishment of a dynamical equilibrium between the bacillus and the host's immune system, which allows the survival of the former inside the latter. When this happens, newly infected individuals become latently infected, because despite harboring the bacteria in their blood, neither becomes sick nor is able to infect others.

On the other hand, after a certain period of time (which may be several years) and usually following an episode of immunosuppression, the balance between the bacterium and its host can be broken. In this case, the bacteria grow and the individual falls ill beginning to develop the clinical symptoms of the disease at rate $k(t)$. Also, latently infected individuals who did not receive effective chemoprophylaxis can be reinfected (exogenously) through a contact with an infectious subject with the same transmission rate $\beta(t)$. In addition, if the infection attacks the lungs (pulmonary TB), the bacillus is present in the sputum, making the guest infectious. After receiving an effective therapy, infectious can spontaneously recover from the disease. Infectious who did not received effective therapy can naturally recover and will be moved to the latently infected class. Recovered individuals can only have partial immunity, and hence, they can undergo a reactivation of the disease.

The flow diagram of the model is presented in Figure 1.

Table 1. Numerical values for the parameters of model system (1).

Parameters	Description	Estimate	Source
Λ	Recruitment rate	397800 individuals$/yr$	Estimated
$\beta(t)$	Transmission rate	To be estimated	
p	Fast route to active TB	0.015	Styblo (1986)
σ	Reinfection parameter	0.7	Assumed
$k(t)$	Slow route to active TB class	To be estimated	
μ	Natural mortality	$0.019896/yr$	NIS (2007)
d	TB mortality of infectious	$0.0575/yr$	NCFAT (2001)
r_1	Chemoprophylaxis rate	$0.001/yr$	NCFAT (2001)
α	Recovery rate of infectious	$0.7311/yr$	NCFAT (2001)
θ	Natural recovery	$0.1828/yr$	Assumed
γ	Relapse of recovered individuals	$0.0986/yr$	NCFAT (2001)

The dynamics of the disease, in a well-mixed population, is then described by the following system of nonlinear non autonomous differential equations:

$$\begin{cases} \dot{S} = \Lambda - \lambda(t)S - \mu S, \\ \dot{E} = (1-p)\lambda(t)S + \theta I - \sigma(1-r_1)\lambda(t)E - A_1(t)E, \\ \dot{I} = p\lambda S + \gamma R + (1-r_1)(k(t) + \sigma\lambda(t))E - A_2 I, \\ \dot{R} = \alpha(1-\theta)I - A_3 R, \end{cases} \tag{1}$$

where

$$\begin{aligned} A_1(t) &= \mu + k(t)(1-r_1), \\ A_2 &= \mu + d + \theta + \alpha(1-\theta), \text{ and} \\ A_3 &= \mu + \gamma. \end{aligned}$$

In Equation (1), $\lambda(t) = \beta(t)I/N$ is the force of the infection; $\beta(t)$ is the effective contact rate of infectious that is sufficient to transmit the infection to susceptible; Λ is the recruitment (immigration and birth) rate, μ is the natural death rate per capital; d is the rate of disease-related death; r_1 is the chemoprophylaxis rate of latently-infected individuals; $k(t)$ is the transition frequency of latent infection (i.e., the probability that a latently-infected individual becomes infectious); σ is the probability that the bacteria is transmitted to an old host after a contact with an infectious subject; α is the recovery rate of infectious (i.e., the probability that an infectious recovers from the disease after a therapy of treatment); θ is the natural recovery rate (i.e., the probability that an infectious recovers from the disease without a therapy of treatment) and γ is the relapse rate of recovered individuals (i.e., the probability that a recovered individual becomes infectious again).

The TB model (1) was simulated with the parameter values given in Table 1.

2.2. Case of constant parameters

Herein, we analyze model system (1) when parameters are constants. In this case, $\beta(t) = \beta$ and $k(t) = k$ so that model system (1) reduces to

$$\begin{cases} \dot{S} = \Lambda - \lambda S - \mu S, \\ \dot{E} = (1-p)\lambda S + \theta I - \sigma(1-r_1)\lambda(t)E - A_1 E, \\ \dot{I} = p\lambda S + \gamma R + (1-r_1)(k + \sigma\lambda(t))E - A_2 I, \\ \dot{R} = \alpha(1-\theta)I - A_3 R, \end{cases} \tag{2}$$

where $A_1 = \mu + k(1-r_1)$, $A_2 = \mu + d + \theta + \alpha(1-\theta)$ and $A_3 = \mu + \gamma$.

2.2.1. *Basic properties*

For model system (2) to be epidemiologically meaningful, it is important to prove that all its state variables are non-negative for all time. In other words, solutions of model system (2) with positive initial data have to remain positive for all time $t > 0$. This can be verified as follows. Suppose, for example, the variable I becomes zero for some time $\bar{t} > 0$, i.e., $I(\bar{t}) = 0$, while all other variables are positive. Then, from the I equation we have $dI(\bar{t})/dt > 0$. Thus, $I(t) \geq 0$ for all $t > 0$. Similarly, it can be shown that the remaining variables are also positive for all time $t > 0$.

Now, we will show that all feasible solutions are uniformly-bounded in a proper subset of Ω. Let $(S, E, I, R) \in \mathbb{R}^4_+$ be any solution of model system (2) with non-negative initial conditions. Adding all equations in the differential system (2) yields

$$\dot{N} = \Lambda - \mu N - dI.$$

Thus, we can deduce that $\dot{N}(t) \leq \Lambda - \mu N(t)$. Now, using Gronwall Lemma, it then follows that $\lim\limits_{t\to+\infty} N(t) \leq \dfrac{\Lambda}{\mu}$, which implies that the trajectories of model system (2) are bounded. On the other hand, from the differential inequality $\dot{N}(t) \leq \Lambda - \mu N(t)$, one can deduce that $N(t) \leq N(0)e^{-\mu t} + \dfrac{\Lambda}{\mu}(1 - e^{-\mu t})$. In particular $N(t) \leq \dfrac{\Lambda}{\mu}$ if $N(0) \leq \dfrac{\Lambda}{\mu}$. Therefore, all feasible solutions of the components of model system (2) enters the region:

$$\Omega = \left\{ (S, E, I, R) \in \mathbb{R}^4_+, \quad N(t) \leq \frac{\Lambda}{\mu} \right\}. \tag{3}$$

Hence, the region Ω, of biological interest, is positively-invariant under the flow induced by model system (2). Further, it can be shown using the theory of permanence (Hutson et al. (1992)) that all solutions on the boundary of Ω will eventually enter the interior of Ω. Furthermore, in Ω, the usual existence, uniqueness and continuation results hold for model system (2). Hence, model system (2) is well posed mathematically and epidemiologically and it is sufficient to consider the dynamics of the flow generated by model system (2) in Ω.

2.2.2. *Local stability of the disease-free equilibrium (DFE)*

For the analysis of the infection's spread, the so-called disease-free equilibrium is particularly relevant. By definition, this is obtained by taking $I = 0$ in equations of model system (2) at the

equilibrium. Then, the disease-free equilibrium is given by $Q_0 = \left(\frac{\Lambda}{\mu}, 0, 0, 0\right)$.

Linearizing all equations in model system (2) around the disease-free equilibrium, the Jacobian matrix of the system is

$$J = \begin{pmatrix} -\mu & 0 & -\beta & 0 \\ 0 & -A_1 & \beta(1-p)+\theta & 0 \\ 0 & k(1-r_1) & \beta p - A_2 & \gamma \\ 0 & 0 & \alpha(1-\theta) & -A_3 \end{pmatrix}.$$

Since $-\mu < 0$, the triangular structure of the Jacobian matrix implies that its stability is associated with the stability of the following submatrix:

$$J_0 = \begin{pmatrix} -A_1 & \beta(1-p)+\theta & 0 \\ k(1-r_1) & \beta p - A_2 & \gamma \\ 0 & \alpha(1-\theta) & -A_3 \end{pmatrix}.$$

Now let

$$A = -A_1,\ B = [\beta(1-p)+\theta\ 0],\ C = \begin{bmatrix} k(1-r_1) \\ 0 \end{bmatrix} \text{ and } D = \begin{bmatrix} \beta p - A_2 & \gamma \\ \alpha(1-\theta) & -A_3 \end{bmatrix}.$$

Then, using the result in Kamgang et al. (2005) on the computation of the eigenvalues of any given matrix of dimension n, the stability of the submatrix J_0 is associated with the stability of the following matrix of dimension 2:

$$J_1 = D - CA^{-1}B = \begin{bmatrix} \beta p - A_2 + \dfrac{k(1-r_1)}{A_1}[\beta(1-p)+\theta] & \gamma \\ \alpha(1-\theta) & -A_3 \end{bmatrix}.$$

The submatrix J_1 is stable if its trace is negative and its determinant non-negative. Therefore, a sufficient condition for this equilibrium to be unstable is given by

$$\frac{\beta(\mu+\gamma)[p\mu + k(1-r_1)]}{(\mu+\gamma)[\mu(\mu+d+\theta)+k(1-r_1)(\mu+d)]+\mu\alpha(1-\theta)[\mu+k(1-r_1)]} \leq 1. \tag{4}$$

Model of this type demonstrates clear infection threshold. In the presence of a threshold, disease eradication requires the reduction of the infection rate below a critical level where a stable infection-free equilibrium is guaranteed. In epidemiological terminology, the infection threshold may be expressed in terms of the basic reproductive number $\mathcal{R}_0$, the average number of infections produced by a single infected individual in a population of susceptibles. From this definition, it is clear that TB infection cannot spread in a population only if $\mathcal{R}_0 < 1$. It then follows that the basic reproduction number $\mathcal{R}_0 < 1$ is given by

$$\mathcal{R}_0 = \frac{\beta(\mu+\gamma)[p\mu + k(1-r_1)]}{(\mu+\gamma)[\mu(\mu+d+\theta)+k(1-r_1)(\mu+d)]+\mu\alpha(1-\theta)[\mu+k(1-r_1)]}. \tag{5}$$

In conclusion, crossing the threshold reduces the basic reproductive number $\mathcal{R}_0$ below unity and the infection is prevented from propagating.

Figure 2 shows the effects of the chemoprophylaxis rate r_1 and the treatment rate α on the basic reproduction number $\mathcal{R}_0$ when $k = 0.00013$ and $\beta = 6$. All other parameter values are fixed as in

Table 1. As expected, when r_1 is fixed, the basic reproduction number, $\mathcal{R}_0$, decreases as α increases and vice versa. Then, combining the chemoprophylaxis of latently infected individuals and treatment of infectious can reduced $\mathcal{R}_0$ to less than unity. Therefore, the best control strategy will be the chemoprophylaxis of latently infected individuals and treatment of infectious or a combination of chemoprophylaxis and treatment.

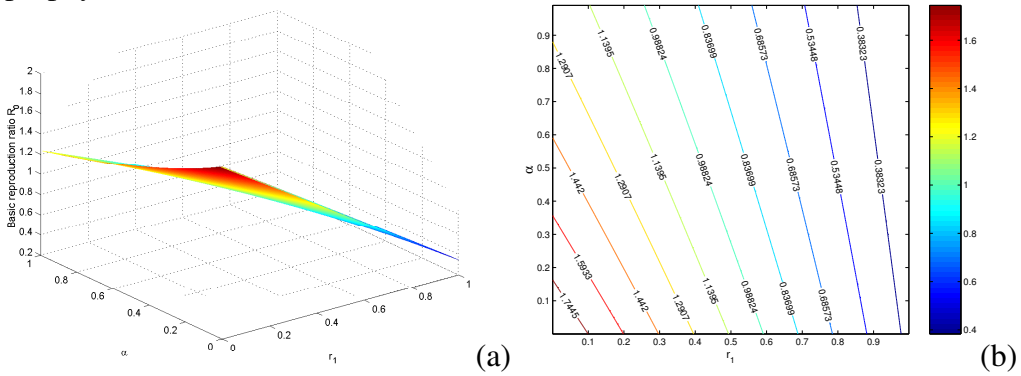

Figure 2. Graphs of the basic reproduction number $\mathcal{R}_0$ of model system (2) in dependence of r_1 and α when $k = 0.00013$ and $\beta = 6$. All other parameter values are as in Table 1.

2.2.3. *Equilibria and bifurcation analysis*

Herein, we investigate the number of equilibrium solutions that model system (2) can have. To this end, let $Q^* = (S^*, E^*, I^*, R^*)$ be any arbitrary equilibrium of model system (2). To find conditions for the existence of an equilibrium for which tuberculosis is endemic in the population (steady state with I^* non zero), the Equations in model system (2) are set to zero, i.e.,

$$\begin{cases} \Lambda - \lambda^* S^* - \mu S^* = 0, \\ (1-p)\lambda^* S^* - \sigma(1-r_1)\lambda^* E^* + \theta I^* - A_1 E^* = 0, \\ p\lambda^* S^* + \sigma(1-r_1)\lambda^* E^* + k(1-r_1)E^* + \gamma R^* - A_2 I^* = 0, \\ \alpha(1-\theta)I^* - A_3 R^* = 0, \end{cases} \tag{6}$$

where

$$\lambda^* = \beta \frac{I^*}{N^*}, \tag{7}$$

is the force of infection at the steady state. Solving the above equations in (6) at the steady state gives

$$\begin{aligned} S^* &= \frac{\Lambda}{\mu + \lambda^*}, \qquad E^* = \frac{\Lambda\lambda^*[(1-p)(\beta\mu + d\lambda^*) + \theta(\mu + \lambda^*)]}{(\mu + \lambda^*)(\beta\mu + d\lambda^*)[A_1 + \sigma(1-r_1)\lambda^*]}, \\ I^* &= \frac{\Lambda\lambda^*}{\beta\mu + d\lambda^*} \qquad \text{and} \qquad R^* = \frac{\alpha\Lambda(1-\theta)\lambda^*}{A_3(\beta\mu + d\lambda^*)}. \end{aligned} \tag{8}$$

Substituting Equation (8) into Equation (7), it can be shown that the non-zero equilibria of system (2) satisfy the following quadratic equation in terms of λ^*:

$$a_2(\lambda^*)^2 + a_1(\lambda^*) + a_0 = 0, \tag{9}$$

where

$$a_2 = \sigma(1-r_1)[\mu+\gamma+\alpha(1-\theta)],$$

$$a_1 = \sigma(1-r_1)[\mu[\mu+d+\alpha(1-\theta)+\gamma(\mu+d)-\beta(\mu+\gamma)]+(\mu+\gamma)(\mu+d+\theta-pd) \\ +\mu\alpha(1-\theta)+k(1-r_1)[\mu+\gamma+\alpha(1-\theta)],$$

$$a_0 = (\mu+\gamma)[\mu(\mu+d+\theta)+k(1-r_1)(\mu+d)]+\mu\alpha(1-\theta)[\mu+k(1-r_1)](1-\mathcal{R}_0).$$

Thus, positive endemic equilibria Q^* are obtained by solving for λ^* from the quadratic Equation (9) and substituting the result (positive values of λ^*) into the expressions of S^*, E^*, I^* and R^* given in Equation (8). Clearly, the coefficient a_2 in Equation (9) is always positive, and a_0 is positive or negative depending whether $\mathcal{R}_0$ is less than or greater than unity, respectively. Thus, the number of possible real roots of the polynomial (9) depends on the signs of a_2, a_1 and a_0. Then, the following result follows:

Lemma 2.1.

Model system (2) has

(i) a unique endemic equilibrium when $a_0 < 0$, i.e., $\mathcal{R}_0 > 1$,
(ii) a unique endemic equilibrium when $a_1 < 0$, and $a_0 = 0$ or $a_1^2 - 4a_2a_0 = 0$,
(iii) two endemic equilibria when $a_0 > 0$, $a_1 < 0$ and $a_1^2 - 4a_2a_0 > 0$;
(iv) no endemic equilibria in all other cases.

It should be pointed out that the case (iii) indicates the possibility of a backward bifurcation (where a locally asymptotically stable DFE co-exists with a locally asymptotically stable endemic equilibrium when $\mathcal{R}_0 < 1$ (see, for instance, Dushoff et al. (1998) and Brauer (2004)) in the TB model (2) when $\mathcal{R}_0 < 1$. To check for this, the discriminant $a_1^2 - 4a_2a_0$ is set to zero and solved for the critical value of $\mathcal{R}_0$, denoted by $\mathcal{R}_c$, given by

$$\mathcal{R}_c = 1 - \frac{a_1^2}{4a_2\mathcal{R}^*}, \tag{10}$$

where $\mathcal{R}^* = (\mu+\gamma)[\mu(\mu+d+\theta)+k(1-r_1)(\mu+d)]+\mu\alpha(1-\theta)[\mu+k(1-r_1)]$. Thus, the backward bifurcation would occur for values of $\mathcal{R}_0$ such that $\mathcal{R}_c < \mathcal{R}_0 < 1$. This is explored below via numerical simulations.

The backward bifurcation phenomenon is illustrated by simulating model system (2) with the parameter values of Table 1. The associated backward bifurcation diagram is depicted in Figure 3.

The time series of model system (2) when $k = 0.00013$ and $\beta = 0.6$ (so that $\mathcal{R}_0 = 0.1363$) is shown in Figure 4. This clearly shows that for the case $\mathcal{R}_0 < 1$, the profiles can converge to either the disease-free equilibrium or an endemic equilibrium point, depending on the initial sizes of the population of the model (owing to the phenomenon of backward bifurcation). It is worth stating that, for the set of parameter values used, the simulations have to be run for a long-time period (in hundred of years).

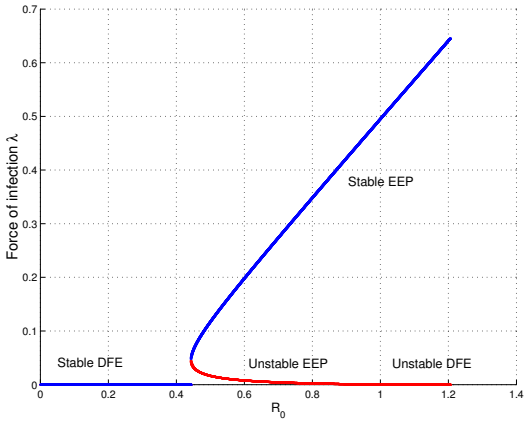

Figure 3. Bifurcation diagram for model system (2) when $k = 0.00013$. The notation EEP stands for endemic equilibrium point. All other parameter values are as in Table 1.

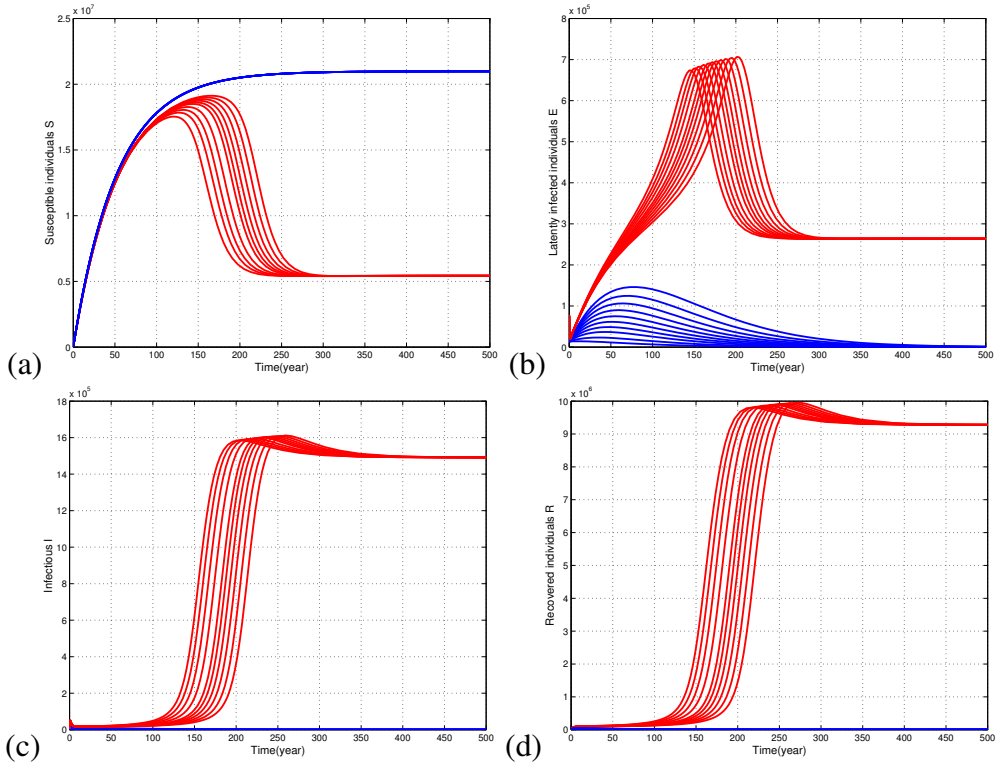

Figure 4. Simulation of model system (2). Time series of (a) susceptible individuals, (b) latently infected individuals, (c) infectious and (d) recovered individual when $k = 0.00013$ and $\beta = 0.6$ (so that $\mathcal{R}_0 = 0.1363$). All other parameter values are as in Table 1.

The epidemiological significance of the phenomenon of backward bifurcation is that the classical requirement of $\mathcal{R}_0 < 1$ is, although necessary, no longer sufficient for disease eradication. In such a scenario, disease elimination would depend on the initial sizes of the population (state variables) of the model. That is, the presence of backward bifurcation in the TB transmission model (2) suggests that the feasibility of controlling TB when $\mathcal{R}_0 < 1$ could depend on the initial sizes of the population. It is important to point out that when there is no exogenous reinfections in the host

population, that is, $\sigma = 0$ in model system (2), model system (2) has a unique endemic equilibrium. Hence, in this case (with $\sigma = 0$), no endemic equilibrium exists whenever $\mathcal{R}_0 \leq 1$. It then follows that, owing to the absence of multiple endemic equilibria for model system (2) with $\sigma = 0$ and $\mathcal{R}_0 \leq 1$, a backward bifurcation is unlikely for model system (2) with $\sigma = 0$ and $\mathcal{R}_0 \leq 1$.

3. Parameter Estimation

One of the most important problems in epidemiology is to reconcile the available data with the mathematical model. Indeed, in most epidemiological models discussed in the literature, the question of estimating unknown parameters has not been played a central role. In the sequel, we will try to evaluate the periodic functions $k(t)$ and $\beta(t)$ by using only real data of Cameroon.

From the National Committee for Fight against Tuberculosis in Cameroon (NCFAT (2001)), we have obtained quarterly numbers of newly reported TB cases from January 2003 to December 2007. The quarterly reported TB cases in Cameroon from 2003 and 2007 show an obvious seasonal fluctuation, with a seasonality peak in the first quarter of each year. This seasonal trend may be mainly attributed to increase times spent in overcrowded, poorly ventilated housing conditions (Schaaf et al. (1996), Rios et al. (2000), Altizer et al. (2006)), and/or more frequent viral infections, which immunological deficiency leading to reactivation of the M. tuberculosis (see for instance Rios et al. (2000)).

The quarterly reported new TB cases in Cameroon from 2003 to 2007 are given in Table 2.

Table 2. The numbers of quarterly reported new TB cases.

Quarter	2003	2004	2005	2006	2007
First quarter	3032	2875	3334	3703	3491
Second quarter	2778	2854	3323	3626	3160
Third quarter	2475	2655	3187	3171	3157
Four quarter	2624	3122	3325	3315	3208

The quarterly numbers of new TB cases in Table 2 correspond to the term:

$$f(t) = \lambda(t)pS(t) + (1 - r_1)[k(t) + \sigma\lambda(t)]E(t), \tag{11}$$

in the third equation of model system (1).

Since the variables and parameters in model system (1) are continuous functions o the time f t, we use trigonometric functions to fit $f(t)$ as a periodic function with five years of observation. Then, using the least-squares trigonometric of the software Mathematica, one has

$$\begin{aligned} f(t) \approx\ & 3120.75 - 232.102\cos(2\pi t/5) + 44.9921\cos(4\pi t/5) \\ & +37.0004\cos(6\pi t/5) - 32.8381\cos(8\pi t/5) + 179\cos(10\pi t/5) \\ & +19.7421\cos(12\pi t/5) - 68.5405\cos(14\pi t/5) - 313.023\sin(2\pi t/5) \\ & -63.8465\sin(4\pi t/5) - 54.4061\sin(6\pi t/5) - 47.7114\sin(8\pi t/5) \\ & +14.7\sin(10\pi t/5) - 29.9372\sin(12\pi t/5) + 12.4314\sin(14\pi t/5). \end{aligned} \tag{12}$$

The comparison of the data with the curve is shown in Figure 5. It clearly appears that the data and the curve match quite well.

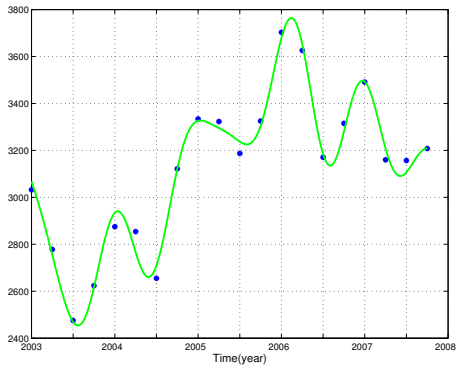

Figure 5. The quarterly numbers of new TB cases and its fitted curve.

After simulations and comparisons, the infection rate $\beta(t)$ and the reactivation rate $k(t)$ have been chosen to be $\beta(t) = \beta_0\beta_1(t)$ and $k(t) = k_0k_1(t)$, respectively, where $\beta_1(t)$ and $k_1(t)$ are the before following two periodic functions:

$$\begin{aligned}\beta_1(t) \approx\ & 2.6006 - 0.1934\cos(2\pi t/5) + 0.0375\cos(4\pi t/5) + 0.0308\cos(6\pi t/5)\\ & -0.0274\cos(8\pi t/5) + 0.1492\cos(10\pi t/5) + 0.0165\cos(12\pi t/5)\\ & -0.0571\cos(14\pi t/5) - 0.2609\sin(2\pi t/5) - 0.0532\sin(4\pi t/5)\\ & -0.0453\sin(6\pi t/5) - 0.0398\sin(8\pi t/5) + 0.0122\sin(10\pi t/5)\\ & -0.0249\sin(12\pi t/5) + 0.0104\sin(14\pi t/5),\end{aligned} \tag{13}$$

and

$$\begin{aligned}k_1(t) \approx\ & (10^{-5})[9.3125 - 0.6926\cos(2\pi t/5) + 0.1343\cos(4\pi t/5) + 0.1104\cos(6\pi t/5)\\ & -0.098\cos(8\pi t/5) + 0.5343\cos(10\pi t/5) + 0.0589\cos(12\pi t/5)\\ & -0.2045\cos(14\pi t/5) - 0.9341\sin(2\pi t/5) - 0.1905\sin(4\pi t/5)\\ & -0.1624\sin(6\pi t/5) - 0.1424\sin(8\pi t/5) + 0.0439\sin(10\pi t/5)\\ & -0.0893\sin(12\pi t/5) + 0.0371\sin(14\pi t/5)].\end{aligned} \tag{14}$$

Note that β_0 and k_0 are related to the magnitudes of the seasonal fluctuation. After simulations and comparisons, we choose $\beta_0 = 0.01$ and $k_0 = 0.133$. In the sensitive analysis, those two parameters are varied to see the influences of the infection rate and the reactivation rate on the new TB case numbers. All other parameter values in the simulations are as in Table 1.

Substituting those values of parameters and functions into model system (1), we obtain the following TB transmission model to simulate TB infection in Cameroon:

$$\begin{cases}\dot{S} = 397800 - \beta_0\beta_1(t)\dfrac{SI}{N} - 0.019896S,\\ \dot{E} = 0.9855\beta_0\beta_1(t)\dfrac{SI}{N} + 0.1828I - 24.9755\beta_0\beta_1(t)\dfrac{EI}{N} - 0.999k_0k_1(t)E - 0.019896E,\\ \dot{I} = 0.015\beta_0\beta_1(t)\dfrac{SI}{N} + 0.0986R + 0.999k_0k_1(t)E + 24.975\beta_0\beta_1(t)\dfrac{EI}{N} - 0.8577I,\\ \dot{R} = 0.5975I - 0.1185R.\end{cases} \tag{15}$$

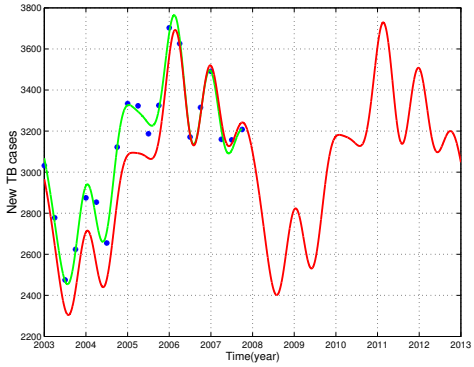

Figure 6. New TB cases: reported number and simulation curve.

We take the first quarter of 2003 as the start time of our simulation. The statistics of the National Institute of Statistics (NIS (2007)) show that the total population of the whole Cameroonian population in 2003 is $N(0) = 15,685,000$. According to the National Committee of Fight against Tuberculosis in Cameroon (NCFAT (2001)), the number of new and relapse cases of TB was 3650, then we take $I(0) = 3,650$. We assume that 70% of the Cameroonian population is infected with *Mycobacterium Tuberculosis*, that is, $S(0) = 4,705,500$. From the average age of the active TB cases, the death rate, and the life expectation, we get the estimation that $R(0) = 2,669$. Then, the direct computation implies that $E(0) = 10,973,681$.

The simulation results are reported in Figure 6 and Figure 7.

Figure 6 illustrates the comparison of the quarterly reported data and the simulation curve of new TB cases in Cameroon. The stars in the curve stand for the reported new TB cases, from January 2003 to December 2007. The simulation result based on our model exhibits the seasonal fluctuation and matches the data with some small error between 2003 and 2005 but after 2005 the model matches the data well. In fact, the dynamics of the suggested TB model is in a transient period between 2003 and 2005. This can be due to the choice of the initial conditions which may not be the exact initial conditions corresponding to the first quarter of 2003. To resolve this problem, we need more data.

Figure 7 gives the trends of susceptible, latently-infected, infectious and recovered individuals in the future several years, respectively.

Sensitivity analysis of parameters is not only critical to model verification and validation in the process of model development and refinement, but also provide insight to the robustness of the model results when making decisions (Saltelli et al. (2000)).

Figure 8 illustrates the impact of β_0 and k_0 on the quarterly new TB cases. From this figure, one can see that β_0 and k_0 have evident impacts on the number of new TB cases. The number of new TB cases increases substantially with a rise in β_0 and k_0, and fails with a decrease in β_0 and k_0.

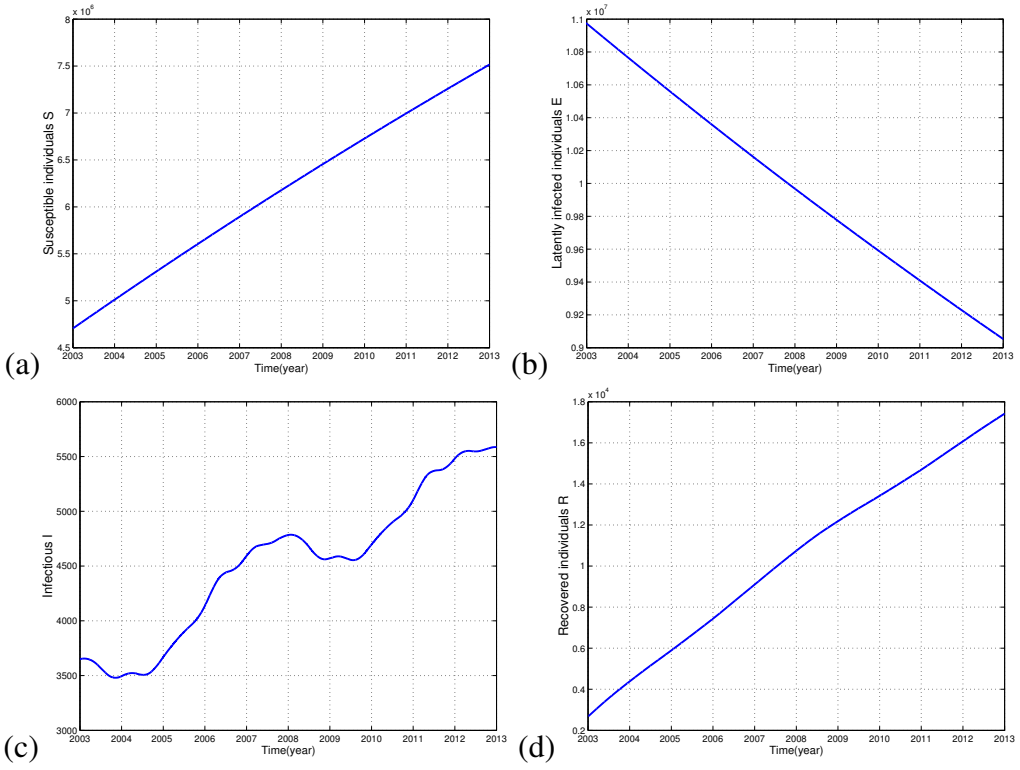

Figure 7. Simulation of model system (1) performed with $\beta_0 = 0.01$ and $k_0 = 0.133$. Time series of (a) susceptible individuals, (b) latently infected individuals, (c) infectious and (d) recovered individuals. All other parameter values are as in Table 1.

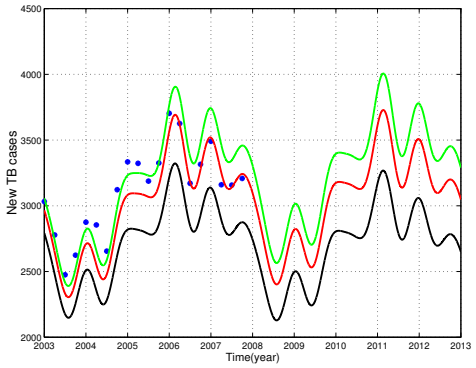

Figure 8. The relationship between new TB cases for different values of β_0 and k_0. In the green-line curve $\beta_0 = 0.0105$ and $k_0 = 0.134$ and in black-line curve $\beta_0 = 0.009$ and $k_0 = 0.132$. Here, the stars correspond to the real data from Cameroon and the red-line curve stands for $\beta_0 = 0.01$ and $k_0 = 0.133$.

4. Optimal Intervention Strategies

Several kinds of interesting nonlinear dynamics behavior of model system (1) such as the backward bifurcation and seasonal patterns have been studied in the previous sections. Since, the backward bifurcation is due to exogenous reinfections, it is then desirable to reduce the exogenous reinfections and failure of treatment in model system (1) so that the number of latently infected individuals

that may develop an active TB will become lower. This is the aim of this section.

4.1. Optimal control problem

Two intervention methods, called controls, are now included in model system (1). Controls are represented as functions of time $u(t)$ and $v(t)$ and assigned reasonable upper and lower bounds. First, $u(t)$ represents the effort on the chemoprophylaxis parameter (r_1) of latently infected individuals to reduce the number of individuals that may become infectious. Second, $v(t)$ is the effort on treatment (r_2) of infectious to increase the number of recovered individuals, i.e., to reduce the number of infectious.

Using the same parameter and class names as in model system (1), the system of differential equations describing our model with controls is

$$\begin{cases} \dot{S} = \Lambda - \lambda(t)S - \mu S, \\ \dot{E} = \lambda(t)(1-p)S + \theta I - (1-ur_1)[k(t)+\sigma\lambda(t)]E - \mu E, \\ \dot{I} = \lambda(t)pS + \gamma R + (1-ur_1)[k(t)+\sigma\lambda(t)]E - v\alpha(1-\theta)I - (\mu+d)I, \\ \dot{R} = v\alpha(1-\theta)I - A_3R, \end{cases} \tag{16}$$

where $\lambda(t)$ and A_3 are defined as in model system (1). Thus, the optimal control objective is to solve the following tracking problem. A control scheme is assumed to be optimal if it minimizes the objective functional:

$$J(u,v) = \int_0^T [B_1 I(t) + B_2 u^2(t) + B_3 v^2(t)]dt, \tag{17}$$

where B_1, B_2 and B_3 are balancing coefficients transforming the integral into the price in Euros expended over a finite time period T in years. The expressions under the integral are costs for implementation of the two controls. Quadratic expressions of the controls are included to indicate non-linearly potentially arising at high treatment levels. We assume that there are practical limitations on the maximum rate at which individuals who may treated via chemoprophylaxis or therapy in a given time period and we define positive constants $u_{\max}$ and $v_{\max}$ accordingly.

Pontryagin's Maximum principle (Pontryagin et al. (1967)) introduces adjoints functions that allow us to attach our state system, i.e., S, E, I and R differential equations, to our objective functional. After first showing the existence of optimal controls (see Fleming et al. (1975)), this principle can be used to obtain differential equations for the adjoint variables, the corresponding boundary conditions and the characterization of an optimal control double u^* and v^*. This characterization gives a representation of an optimal control in terms of the state and adjoint functions. Also, this principle converts the problem of minimizing the objective functional subject to the state system into minimizing the Hamiltonian with respect to the controls (bounded measurable functions) at each time t.

4.2. Characterization of optimal controls

We invoke Pontryagin's Maximum Principle (Pontryagin et al. (1967)) to determine the precise formulation of our optimal controls $u^*(t)$ and $v^*(t)$. To do this, we note that our Hamiltonian is

given by

$$\begin{aligned} H &= B_1 I(t) + B_2 u^2(t) + B_3 v^2(t) + w_S[\Lambda - \lambda(t)S(t) - \mu S(t)] \\ &\quad + w_E[\lambda(t)(1-p)S(t) + \theta I(t) - (1-u(t)r_1)[k(t)+\sigma\lambda(t)]E(t) - \mu E(t)] \\ &\quad + w_I[\lambda(t)pS(t) + \gamma R(t) + (1-u(t)r_1)[k(t)+\sigma\lambda(t)]E(t) \\ &\quad - v(t)\alpha(1-\theta)I(t) - (\mu+d)I(t)] + w_R[v(t)\alpha(1-\theta)I(t) - A_3 R(t)], \end{aligned} \tag{18}$$

where w_S, w_E, w_I and w_R are the adjoint functions associated with their respective states. Note that in H, each adjoint function multiplies the right-hand side of the differential equation of its corresponding state function. The first terms in H come from the integrand of the objective functional. Thus, the adjoint variable w_j, $j = S, E, I$ together with our state system determine our optimality system.

Pontryagin's Maximum Principle states that the unconstrained optimal controls u^* and v^* satisfy

$$\frac{\partial H}{\partial u} = 0 \qquad \text{and} \qquad \frac{\partial H}{\partial v} = 0,$$

whenever $0 < u^*(t) < u_{\max}$ and $0 < v^*(t) < v_{\max}$, and taking the bounds into account. So, we find $\dfrac{\partial H}{\partial u}$ and $\dfrac{\partial H}{\partial v}$ by setting our partial derivatives of H equal to zero. Thus, one obtains, in compact form:

$$u^*(t) = \min(u_{\max}, \max(\hat{u}(t), 0)) \qquad \text{and} \qquad v^*(t) = \min(v_{\max}, \max(\hat{v}(t), 0)), \tag{19}$$

where

$$\hat{u} = \frac{r_1(w_I - w_E)[k(t)+\sigma\lambda(t)]E(t)}{2B_2} \qquad \text{and} \qquad \hat{v} = \frac{\alpha(1-\theta)(w_I - w_R)I(t)}{2B_3}.$$

4.3. Derivation of the optimality system

Getting the optimality system is an important part of this problem. It describes mathematically how the system behaves under the application of the controls. Therefore, we may find how the different populations of susceptible, latently-infected, infectious and recovered individuals decay or grow when latently infected individuals and infectious are treated with optimal chemoprophylaxis and therapy as characterized in the previous subsection.

The optimality system is defined as the state system together with the adjoint system and the optimal controls u^* and v^*. The adjoint system is given by

$$\frac{dw_S}{dt} = -\frac{\partial H}{\partial S}, \qquad \frac{dw_E}{dt} = -\frac{\partial H}{\partial E}, \qquad \frac{dw_I}{dt} = -\frac{\partial H}{\partial I} \qquad \text{and} \qquad \frac{dw_R}{dt} = -\frac{\partial H}{\partial R}.$$

Then, given an optimal control double (u^*, v^*) and the corresponding states (S^*, E^*, I^*, R^*), there

exists adjoint functions satisfying:

$$\begin{aligned}
\frac{dw_S}{dt} &= \beta(t)\frac{I(N-S)}{N^2}[w_S-(1-p)w_E-pw_I]+\beta(t)\sigma(1-ur_1)(w_I-w_E)\frac{EI}{N^2}+\mu w_S,\\
\frac{dw_E}{dt} &= \beta(t)\frac{SI}{N^2}[-w_S+(1-p)w_E+pw_I]+\beta(t)\sigma(1-ur_1)(w_E-w_I)\frac{I(N-E)}{N^2}\\
&\quad +k(t)(w_E-w_I)(1-ur_1)+\mu w_E,\\
\frac{dw_I}{dt} &= -B_1+\beta(t)\frac{S(N-I)}{N^2}[w_S-(1-p)w_E-pw_I]+\beta(t)\sigma(1-ur_1)(w_E-w_I)\frac{E(N-I)}{N^2}\\
&\quad -\theta w_E+\alpha(1-\theta)v(w_I-w_R)+(\mu+d)w_I,\\
\frac{dw_R}{dt} &= \beta(t)\frac{SI}{N^2}[-w_S+(1-p)w_E+pw_I]+\beta(t)\sigma(1-ur_1)(w_E-w_I)\frac{EI}{N^2}-\gamma w_I+A_3w_R.
\end{aligned} \tag{20}$$

The final component in the optimality system is the set of *transversality conditions*, which in this case reduces to end conditions on the adjoint variables. They are a consequence of the following result, which can also be found in Fleming and Rishel (1975).

Given the maximisation problem $\max J[u] = F(x(T)) + \int_0^T f_0(x,u)dt$, subject to the state system $dx/dt = f(x,t,u)$ and such that $x(T)$ belongs to some *target set* $g(x(T))$, we have the following transversality conditions on the adjoint variables:

$$w_i(T) = \nabla F(x(T)) + \sum_{i=1}^{k} c_i g_i(x(T)). \tag{21}$$

The function F is known as the *terminal cost*.

In our problem, there is no terminal cost, so $F(x(T)) = 0$. We also do not have a target set for our state variables; we have a desired end result, of course, but the final state is in fact free, so the summation term is also zero.

Therefore, the transversality conditions for the adjoint variables are

$$w_S(T) = 0, \qquad w_E(T) = 0, \qquad w_I(T) = 0 \qquad \text{and} \qquad w_R(T) = 0. \tag{22}$$

The state system of the differential equations and the adjoint system of the differential equations together with the control characterization above from the optimality system have to be solved numerically. Since the state equations have initial conditions and the adjoint equations have final time conditions, we cannot solve the optimality system directly by only sweeping forward in time. Thus, an iterative algorithm, "forward-backward sweep method" (see Lenhart et al. (2007)), is used. An initial estimate for the controls is made. The state system is then solved forward in time from the dynamics using a Runge-Kutta method of fourth order. The resulting state values are placed in the right-hand sides of the adjoint differential equations. Then, the adjoint system with the given initial conditions is solved backward in time, again employing a fourth Runge-Kutta method. Both state and adjoint values are used to update the control using the characterization, and then the process is repeated. This iterative process terminates when the current state, adjoint, and control values converge sufficiently.

4.4. Optimal control numerical simulations

Numerical solutions to the optimality system comprising of the state system (16) and the adjoint system (20) are carried out using parameters of Figure 7. The initial conditions have been chosen to be $S(0) = 6,600,000$, $E(0) = 9,600,000$, $I(0) = 4,600$ and $R(0) = 13,000$, which are the number of susceptible, latently-infected, infectious and recovered individuals in 2010 in the mainland of Cameroon (predicted by our numerical study in Figure 7) as the start time of simulation. With this strategy, the controls on chemoprophylaxis u and treatment v are optimized, with weight factor $B_1 = 75$ Euro per year of the therapy, $B_2 = 15$ Euro (per proportion of E treated)^2 and $B_3 = 10$ Euro (per proportion of I treated)^2. Also, we take $u_{\max} = v_{\max} = 1$. Cost coefficients are fixed within the integral expression (17) and the optimal schedule of the two controls over $T = 5$ year is simulated.

Numerical simulations are depicted in Figure 9 and Figure 10. One can see from Figure 9, that the optimal chemoprophylaxis and drug treatment protocol have a very desirable effect upon the population of infectious which decreases for almost the entire length of treatment.

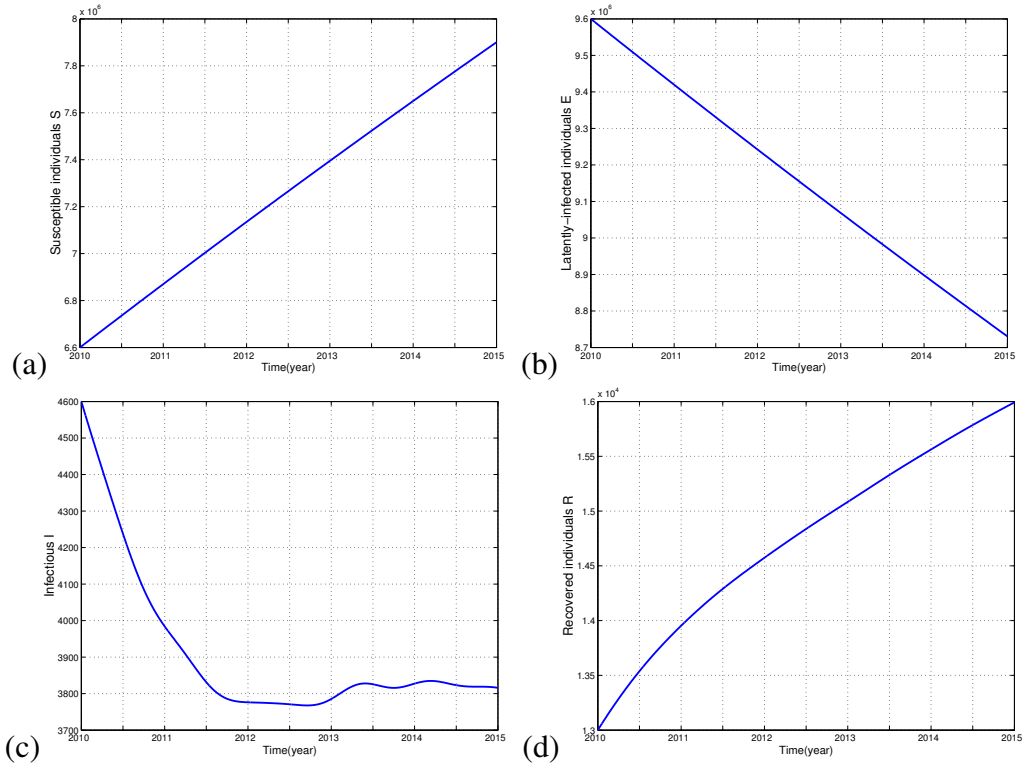

Figure 9. Dynamics of model system (16) showing the effect of chemoprophylaxis and treatment rates on the host population. Time series of (a) susceptible individuals, (b) latently infected individuals, (c) infectious and (d) recovered individuals. All other parameter values are as in Figure 7.

As Figure 10 illustrates, optimal control results provide clearly different strategies for relative application of chemoprophylaxis of latently-infected individuals and treatment of infectious for the Cameroonian population. From this figure, we can see that the disease chemoprophylaxis control u and the disease treatment control v are at the upper bounds $u_{\max} = 1$ and $v_{\max} = 1$ all through the 5 years of the simulations and drop rapidly at the end. For this population, chemoprophylaxis and

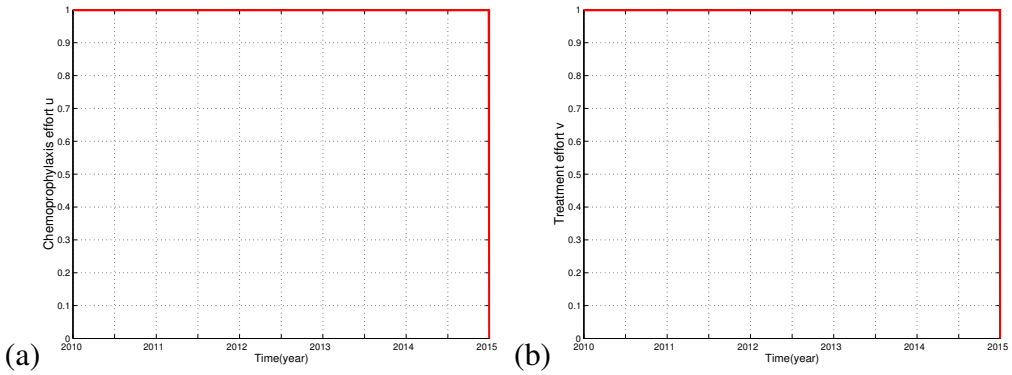

Figure 10. Optimal balance of controls for model system (16). (a) Optimal chemoprophylaxis control u and (b) optimal treatment control v. All other parameter values are as in Figure 7.

treatment greatly reduces death due to disease. Consequently, fewer funds can be allow for chemoprophylaxis in the optimal scheme; however, a temporary maximum treatment is advantageous at the onset of the infection. In combination with other controls, high level of chemoprophylaxis is most beneficial at the beginning of a TB control program to decrease the rate at which latently-infected individuals become infectious, providing more time to effectively implement the treatment. Recall that our analysis on the basic reproduction number revealed that chemoprophylaxis and treatment play a strong role on controlling the total number of infectious.

5. Conclusion

This paper has studied the problem of parameter estimation and optimal control of a comprehensive, continuous deterministic model for the dynamics of transmission of TB within a human community. We first presented a mathematical model that can describe the TB seasonal by incorporating periodic coefficients. The uncontrolled model with constant parameters has been analyzed to gain insight into its qualitative dynamics. We have mainly found that the model with constant parameters exhibits the phenomenon of backward bifurcation, where the stable disease-free equilibrium co-exists with a stable endemic equilibrium, when the basic reproduction number is less than unity. This (backward bifurcation) dynamics feature is caused by the reinfection of latently-infected and recovered individuals. After, we have proposed a numerical study to estimate some parameters of the model from real data of TB in Cameroon.

It has been found that there is a seasonal pattern of new TB cases in the mainland of Cameroon. Throughout numerical simulations, we found that the number of new TB cases is an increasing function of β_0 or k_0 and is more sensitive to k_0 than β_0. An optimal control strategy for the TB model with seasonality has been presented. The proposed optimal control shown the result of optimally controlling exogenous reinfections using chemoprophylaxis and failure of treatment in the reduction of the number of individuals with active TB. However, the control of epidemic systems is not usually an easy task since in real situations it is rather difficult to implement the control policies suggested by the mathematical analysis. Through numerical simulation, we observe that our controls actually remain close to constants soon after initiation of chemoprophylaxis and treatment, and drop rapidly near the end.

We believe that this initial drop is directly dependent upon the action of the recovered which occurs shortly after chemoprophylaxis and treatment initiation in response to the high infection level. That is, our optimal chemoprophylaxis and treatment are actually reduced for a period of time, while the recovered in the host population takes over. This indicates that a better care of infectious by some means other than continuation administration of drugs should be considered seriously in clinical setting.

An important result of this analysis is that a cost-effective balance of chemoprophylaxis and treatment methods can successfully control TB in Cameroon. Treatment strategies such as interruption of drug therapy should also be considered. This can be tested clinically via drug trails, but also mathematically using a periodic control.

REFERENCES

Altizer, S., Dobson, A., Hosseini, P., Hudson, P., Pascual, M. and Rohani, P. (2006). Seasonality and the dynamics of infectious diseases, Ecol. Lett., Vol. 9, pp. 467–484.

Anderson, B.D.O. and Moor, J.B. (1990) *Optimal Control: Linear Quadratic Methods*, Prentice-Hall, NY.

Anderson, R.M. and May, R.M. (1992). *Infectious Diseases of Humans: Dynamics and Control*, Oxford University Press, Oxford, England.

Aron, J.L. and Schwartz, I.B. (1984). Seasonality and period-doubling bifurcations in an epidemic model, J. Theor. Biol., Vol. 110, pp. 665–679.

Bleed, D., Watt, C. and Dye, C. (1982). Epidemiology of tuberculosis, Am. Rev. Respir. Dis., Vol. 125, pp. 8–13.

Bowong, S. (2010). Optimal control of the transmission dynamics of tuberculosis, Nonlinear dynamics, Vol. 61, pp. 729–748. doi:10.1007/s11071-010-9683-9

Bowong, S. and Kurths, J. (2010). Parameter estimation based synchronization for an epidemic model with application to tuberculosis in Cameroon, Phys Lett A, Vol. 374, pp. 449–505.

Brauer, F. (2004). Backward bifurcations in simple vaccination models, J. Math. Ana. Appl., Vol. 298, pp. 418–431.

Colizza, V., Barrat, A., Barthélemy, M. and Vespignani, A. (2006). The role of the airline transportation network in the prediction and predictability of global epidemics, Proc. Natl. Acad. Sci. U.S.A., Vol. 103, pp. 2015–2020.

Daley, D.J. and Gani, J. (1999) *Epidemic Modeling*, Cambridge University Press, Cambridge, England.

Daniel, T., Bates, J. and Downes, K. (1994). *in Tuberculosis: Pathogenesis, Protection, and Control*, edited by B. R. Bloom American Society for Microbiology, Washington, pp. 13–24.

Douglas, A.S., Strachan, D.P. and Maxwell, J.D. (1996). Seasonality of tuberculosis: the reverse of other respiratory diseases in the UK, Thorax, Vol. 51, pp. 944–946.

Dushoff, J., Huang, W. and Castillo-Chavez, C. (1998). Backwards bifurcations and catastrophe in simple models of fatal disease, J. Math. Biol., Vol. 36, pp. 227–248.

Dye, C. and Williams, B.G. (2010). The Population Dynamics and Control of Tuberculosis, Science, Vol. 328, pp. 856–861.

Fleming, W. and Rishel, R. (1975). *Deterministic and stochastic optimal control*, Springer Verlag, New York.

Guimera, R., Mossa, S., Turtschi, A. and Amaral, L.A.N. (2005). The worldwide air transportation network: Anomalous centrality, community structure, and cities global roles, Proc. Natl. Acad. Sci. U.S.A., Vol. 102, pp. 7794–7799.

Hufnagel, L., Brockmann, D. and T. Geisel, T. (2004). Forecast and control of epidemics in a globalized world, Proc. Natl. Acad. Sci. U.S.A., Vol. 101, pp. 15124–15129.

Hutson, V. and K. Schmitt, K. (1992). Permanence and the dynamics of biological systems, Math. Biosci., Vol. 111, pp. 1–71.

Joshi, H.R. (2002). Optimal Control of an HIV Immunology Model, Optimal Control Applications & Methods, Vol. 23, pp. 199–213.

Jung, E. and Feng, Z. (2002). Optimal control of treatments in a two-strain tuberculosis model, Dis. Cont. Dyn. Syst. Series B, Vol. 2, pp. 473–482.

Kamgang, J.C. and Sallet, G. (2008). Computation of threshold conditions for epidemiological models and global stability of the disease-free equilibrium (DFE), Math. Biosc., Vol. 213, pp. 1–12.

Kamien I.M., and Schwartz, N.L. (1991). *Dynamics Optimization*, Advanced Textbooks in Economics V. 31, North-Holland Publishing Co.

Lakshmikantham, V., Leela, S. and Martynyuk, A.A. (1989). *Stability analysis of nonlinear systems*, Marcel Dekker, Inc., New-York and Basel.

Lenhart, S., and J. Workman, J. (2007). *Optimal Control Applied to Biological Models*, Chapman and Hall.

Leung, C.C., Yew, W.W., Chan, T.Y.K., Tam, C.M., Chan, C.Y., Chan, C.K., Tang, N., Chang, K.C. and Law, W.S. (2005). Seasonal pattern of tuberculosis in Hong Kong, Int. J. Epidemiol., Vol. 34, pp. 924–930.

Liu, L., Zhao, X-Q. and Zhou, Y. (2010). A Tuberculosis Model with Seasonality, Bull. Math. Biol., Vol. 72, No. 4, pp. 931–952. doi:10.1007/s11538-009-9477-8.

Miller, R.L., Schaefer, E., Gaff, H., Fister, K.R., and Lenhart, S. (2010). Modeling optimal intervention strategies for cholera, Bul. Math. Biol.,Vol. 72, No. 8, pp. 2004–2018. doi:10.1007/s11538-010-9521-8

Moualeu, D.P., Bowong, S. and Kurths, J. (2013). Parameter estimation of a tuberculosis model in a patchy environment: Case of Cameroon, Biomat, Vol. 2013, pp. 352–373.

Murphy, B.M., Singer, B.H., Anderson, S. and Kirschner, S. (2002). Comparing epidemic tuberculosis in demographically distinct heterogeneous populations, Math. Biosci.,- Vol. 180, pp. 161–185.

Murray, J.D. (2002). *Mathematical Biology*, Springer-Verlag, Berlin, Germany.

Nagayama, N. and Ohmori, M. (2006). Seasonality in various forms of tuberculosis, Int. J. Tuberc. Lung Dis., Vol. 10, pp. 1117–1122.

Narula, P., Piratla, V., Bansal, A., Azad, S. and Lio, P. (2016). Parameter estimation of tuberculosis transmission model using Ensemble Kalman filter across Indian states and union territories, Infect. Disease and Health, Vol. 20, No. 4, pp. 184–191.

National Committee of Fight Against Tuberculosis, (2001). *Guide du personnel de la santé*, Ministère de la santé publique, Cameroon.

National Institute of Statistics, *Evolution des systèmes statistiques nationaux* (Cameroun, 2007).

Pontryagin, L.S., Boltyanskii, V.G., Gamkrelize, R.V. and Mishchenko, E.F. (1967). *The Mathematical Theory of Optimal Processes*, Wiley, New York.

Rios, M., Garcia, J.M., Sanchez, J. A. and Perez, D. (2000). A statistical analysis of the seasonality in pulmonary tuberculosis, Eur. J. Epidemiol., Vol. 16, pp. 483–488.

Saltelli, A., Chan, K. and Scott, M. (2000). *Sensitivity Analysis, Probability and Statistics*, Series. Wiley, New York.

Schaaf, H.S., Nel, E.D., Beyers, N., Gie, R.P., Scott, F. and Donald, P.R. (1996). A decade of experience with Mycobacterium tuberculosis culture from children: a seasonal influence on incidence of childhood tuberculosis, Tuber. Lung Dis., Vol. 77, pp. 43–46.

Styblo, K. (1986). Tuberculosis control and surveillance, in *Recent Advances in Respiratory Medicine* (edited by D. Flenley and T. Petty), London, Vol. 4, pp. 77108–12.

Styblo, K., Meijer, J. and Sutherland, I. (1969). The transmission of tubercle bacilli: Its trend in a human population, Bull. Int. Union Tuberc., Vol. 24, pp. 137–78.

Tanaka, M.M., Francis, A.R., Luciani, F. and Sisson, S.A. (2006). Using approximate Bayesian computation to estimate tuberculosis transmission parameters from genotype data, Genetics, Vol. 173, pp. 1511e20–1511e27.

Thorpe, L.E., Frieden, T.R., Laserson, K.F., Wells, C. and Khatri, G.R. (2004). Seasonality of tuberculosis in India: Is it real and what does it tell us?, Lancet, Vol. 364, pp. 1613–14.

Wang, W. and Ruan, S. (2004). Simulating the SARS outbreak in Beijing with limited data, J. Th. Biol., Vol. 227, pp. 369–379.

Wilson, L. (1990). The historical decline of tuberculosis in Europe and America: its causes and significance, J. Hist. Med. Allied Sci., Vol. 45, pp. 366–396.

World Health Organization (2009). *Global Tuberculosis Control: A Short Update to the 2009 Report*, World Health Organization, Geneva.